



Deliverable Report

Deliverable D1.6

Deliverable Title: Final QPM SPDC

Grant Agreement number: **255914**

Project acronym: **PHORBITECH**

Project title: **A Toolbox for Photon Orbital Angular Momentum Technology**

Project website address: **www.phorbitech.eu**

Name, title and organization of the scientific representative of deliverable's lead beneficiary (task leader):

Dr Juan P. Torres

ICFO - Institut De Ciencies Fotoniques

Castelldefels, Spain

Deliverable table

Deliverable no.	D1.6
Deliverable name	Final QPM SPDC
WP no.	1
Lead beneficiary no.	3 (ICFO)
Nature	R
Dissemination level	PU
Delivery date from Annex I	Month 24
Actual delivery date	30 September 2012

D1.6 Final QPM SPDC: Final analysis of the performances and features of the transverse quasi-phase-matching (QPM) approach for OAM SPDC generation. Quasi-phase-matching will be achieved by modulating the material composition and structure, as well as by tailoring the pump beam transverse profile, and spectral and/or temporal shape. [Excerpt from the GA-Annex I describing the deliverables of WP1, page 8]

1. Previous work described in Deliverable D1.2 (intermediate report)

In the intermediate report delivered at Month 12 (see paper [1] S. Palacios, R. de J. Leon-Montiel, M. Hendrych, A. Valencia and J. P. Torres, *Flux enhancement of photons entangled in orbital angular momentum*, Optics Express **19**, 14108 (2011), corresponding to Deliverable D1.2) we designed high-flux SPDC configurations aimed at generating specific qubit and qutrit states with specific OAM correlations.

For instance, for generating the important state quantum state of the form

$$|\Psi\rangle = \frac{1}{\sqrt{2}} \left(|R; m = +1\rangle_S |L; m = -1\rangle_i + |L; m = -1\rangle_S |R; m = +1\rangle_i \right)$$

where R represents right-handed circularly polarized light, L left-handed circularly polarized light, and $m=+1$ ($m=-1$) an orbital angular momentum mode with the corresponding index and $p=0$, the optimum configuration is given in Fig. 1. In this case, an estimated 82% of all photons generated belong to the Hilbert space of interest.

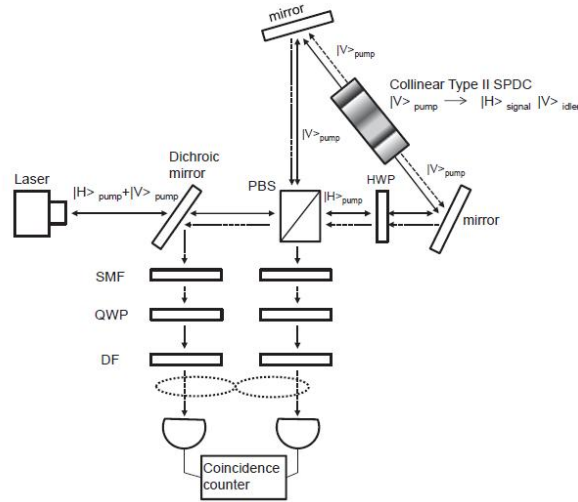


Figure 1: Scheme of the combination of a type-II SPDC source embedded in a Sagnac interferometer and diffractive elements to generate photons entangled in the polarization and spatial degrees of freedom with maximum efficiency. SMF: Single-mode fiber; QWP: Quarter-wave plate; HWP: Half-wave plate; PBS: Polarization beam splitter; DF: Diffractive element. The linked dot lines represent the existence of entanglement. This figure comes from Palacios, Leon-Montiel, M. Hendrych, Valencia and Torres [1].

2. Generation of high entanglement making use of chirped quasi-phase-matching

One of the promises of using the spatial degree of freedom (or Orbital Angular Momentum modes) of two-photon states generated in Spontaneous Parametric Down-Conversion (SPDC) is to produce truly high entanglement, i.e., tens of ebits of entanglement when measured in terms of the entropy of entanglement. One of the advantages of using the spatial degree of freedom over other continuous degrees of freedom that characterize photons, as the frequency, is that there is a myriad of efficient optical tools to generate, control and detect spatial modes.

The amount of spatial entanglement generated depends on the SPDC geometry used (collinear vs non-collinear), the length of the nonlinear crystal (L) and the size of the pump beam (w_0). Under certain approximations, the entropy of entanglement can be shown to be dependent on the ratio L/L_d , where $L_d = kpw_0^2/2$ is the Rayleigh range of the pump beam and k_p is its longitudinal wave-number. Therefore, large values of the pump beam waist w_0 and shorter crystals are ingredients for generating high entanglement [2]. However, the use of shorter crystals also reduces the total flux-rate of generated entangled photon pairs [2]. Moreover, certain applications might benefit from the use of focused pump beams. For instance, for $L = 1$ mm, $w_0 = 200\mu\text{m}$ and $k_p = 15.7\mu\text{m}^{-1}$, one obtains $E \sim 9$. For a longer crystal of $L = 20$ mm, the amount of entanglement is severely reduced to $E \sim 5$ ebits.

We put forward here [3] a scheme to generate massive spatial entanglement, i.e., a staggering large value of the entropy of entanglement, independently of some relevant experimental parameters such as the crystal length or the pump beam waist. This allows to reach even larger amounts of entanglement that possible nowadays with the usual configurations used, or to attain the same amount of entanglement but with other values of the nonlinear crystal length or the pump beam waist better suited for specific experiments. The scheme described below is based on the use of Quasi-phase-matching (QPM) engineering of nonlinear crystals (see Fig. 2).

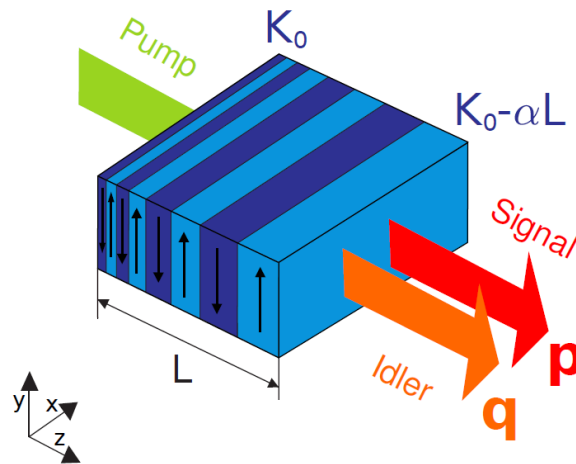


Fig. 2. Scheme of SPDC in a linearly chirped quasi-phase-matched nonlinear crystal. The pump beam is a Gaussian beam, and p and q designate the transverse wave numbers of the signal and idler photons, respectively. K_0 is the grating wave-vector at the input face of the nonlinear crystal, and $K_0 - \alpha L$ at its output face. The signal and idler photons can have different polarizations or frequencies. The different colors (or different direction of arrows) represent domains with different sign of the nonlinear coefficient. This figure comes from Svozilik, Perina and Torres [3].

QPM is a technique that was originally invented [4] to achieve the condition of phase matching between the waves that take part in nonlinear processes such as Second Harmonic Generations or Spontaneous Parametric Down-Conversion (SPDC). In its simplest version, it produces a periodic reversal (with period Λ) of the sign of the nonlinear coefficient of the nonlinear material along the direction of propagation of all interacting waves.

But the capabilities of QPM go beyond making possible phase matching in configurations where phase matching cannot be achieved otherwise. Since present-day technology allows mapping nearly any spatial distribution of signs of the nonlinear coefficient into the nonlinear material, QPM becomes also a tool to tailor the shape in frequency and space of the down-converted photons. In transverse QPM, the sign of the nonlinear coefficient changes in the transverse plane, and it produces spatial shaping of the photons [5].

In the more common longitudinal QPM, the nonlinear coefficient change along the direction of propagation of the waves (z), producing in general, a change of the spectrum of the down-converted [6]. But this type of QPM can also produce spatial tailoring of the down-converted photons, something that even was observed experimentally in [6], its consequences for tailoring spatial entanglement were not fully appreciated. The key point is to realize that when considering a focused pump beam, and the whole spatial shape of the down-converted photons, the phase matching condition depends on the transverse wave number of the signal (p) and idler photons (q), so that

$$k_p(p+q) - k_s(p) - k_i(q) - \frac{2\pi}{\Lambda(z)} = 0$$

where k_s and k_i are the transverse wave numbers of the signal and idler photons, respectively.

Now, by modifying the period Λ along the direction of propagation (chirped QPM), different values of the transverse wave-numbers q_s and q_i might achieve phase matching at different locations of nonlinear crystal. In this way, the decomposition of the spatial quantum state of the down-converted photons into the Orbital Angular Momentum (OAM) modes can be enhanced, producing a corresponding enhancement of the spatial entanglement.

References

- [1] Silvana Palacios, R. de J. Leon-Montiel, Martin Hendrych, Alejandra Valencia and Juan P. Torres, *Flux enhancement of photons entangled in orbital angular momentum*, Optics Express **19**, 14108 (2011).
- [2] S. S. R. Oemrawsingh, X. Ma, D. Voigt, A. Aiello, E. R. Eliel, G. W. 't Hooft, and J. P. Woerdman, *Experimental demonstration of fractional orbital angular momentum entanglement of two photons*, Phys. Rev. Lett. **95**, 240501 (2005).

[3] J. Svozilik, J. Perina and J. P. Torres, *High spatial entanglement via chirped quasi-phase-matched optical parametric down-conversion*, submitted for its publication, also in arXiv:1208.4531 from 22nd August 2012.

[4] J. A. Armstrong, N. Bloembergen, D. Ducuing and P. S. Pershan, Interactions between Light Waves in a Nonlinear Dielectric, *Phys. Rev.* **127**, 1918 (1962).

[5] See the original idea in J. P. Torres, A. Alexandrescu, S. Carrasco and L. Torner, *Quasi-phase-matching engineering for spatial control of entangled two-photon states*, *Opt. Lett.* **29**, 376 (2004), and an experimental implementation in X. Q. Yu, P. Xu, Z. D. Xie, J. F. Wang, H.Y. Leng, J. S. Zhao, S. N. Zhu and N. B. Ming, *Transforming Spatial Entanglement Using a Domain-Engineering Technique*, *Phys. Rev. Lett.* **101**, 233601 (2008).

[6] M. B. Nasr, S. Carrasco, B. E. A. Saleh, A. V. Sergienko, M. C. Teich, J. P. Torres, L. Torner, D. S. Hum, and M.M. Fejer, *Ultrabroadband Biphotons Generated via Chirped Quasi-Phase-Matched Optical Parametric Down-Conversion*, *Phys. Rev. Lett.* **100**, 183601 (2008).

PHORBITECH contribution to this deliverable

PHORBITECH contributed to this deliverable by supporting part of the time of Jiri Svozilik and in the purchase of some lab materials.

PHORBITECH contributors to this deliverable

ICFO: Jiri Svozilik and Juan P. Torres

Publication(s) included in this deliverable:

- J. Svozilik, J. Perina and J. P. Torres, *High spatial entanglement via chirped quasi-phase-matched optical parametric down-conversion*, submitted for publication. Also published online in arXiv:1208.4531.

High spatial entanglement via chirped quasi-phase-matched optical parametric down-conversion

Jiří Svozilik,^{1,2,*} Jan Peřina Jr.,² and Juan P. Torres^{1,3}

¹*ICFO—Institut de Ciències Fòniques, Mediterranean Technology Park, 08860, Castelldefels, Barcelona, Spain*

²*Palacký University, RCPTM, Joint Laboratory of Optics,
17.listopadu 12, 771 46 Olomouc, Czech Republic*

³*Department of Signal Theory and Communications,
Universitat Politècnica Catalunya, Campus Nord D3, 08034 Barcelona, Spain*

(Dated: August 23, 2012)

By making use of the spatial shape of paired photons, parametric down-conversion allows the generation of two-photon entanglement in a multidimensional Hilbert space. How much entanglement can be generated in this way? In principle, the infinite-dimensional nature of the spatial degree of freedom renders unbounded the amount of entanglement available. However, in practice, the specific configuration used, namely its geometry, the length of the nonlinear crystal and the size of the pump beam, can severely limit the value that could be achieved. Here we show that the use of quasi-phase-matching engineering allows to increase the amount of entanglement generated, reaching values of tens of ebits of entropy of entanglement under different conditions. Our work thus opens a way to fulfill the promise of generating massive spatial entanglement under a diverse variety of circumstances, some more favorable for its experimental implementation.

PACS numbers: 03.67.Bg, 03.65.Aa, 42.50.Dv, 42.65.Lm

Entanglement is a genuine quantum correlation between two or more parties, with no analogue in classical physics. During last decades it has been recognized as a fundamental tool in several quantum information protocols, such as quantum teleportation [1], quantum cryptography [2] and quantum key distribution [3], and distributed quantum computing [4].

Nowadays, spontaneous parametric down-conversion (SPDC), a process where the interaction of a strong pump beam with a nonlinear crystal mediates the emission of two lower-frequency photons (signal and idler), is a very convenient way to generate photonic entanglement [5]. Photons generated in SPDC can exhibit entanglement in the polarization degree of freedom [6], frequency [7] and spatial shape [8, 9]. One can also make use of a combination of several degrees of freedom [10, 11].

Two-photon entanglement in the polarization degree of freedom is undoubtedly the most common type of generated entanglement, due both to its simplicity, and that it suffices to demonstrate a myriad of important quantum information applications. But the amount of entanglement is restricted to 1 ebit of entropy of entanglement [12], since each photon of the pair can be generally described by the superposition of two orthogonal polarizations (two-dimensional Hilbert space). On the other hand, frequency and spatial entanglement occurs in an infinite dimensional Hilbert space, offering thus the possibility to implement entanglement that inherently lives in a higher dimensional Hilbert space (qudits).

Entangling systems in higher dimensional systems (frequency and spatial degrees of freedom) is important both for fundamental and applied reasons. For example, noise and decoherence tend to degrade quickly quantum corre-

lations. However, theoretical investigations predict that physical systems with increasing dimensions can maintain non-classical correlations in the presence of more hostile noise [13, 14]. Higher dimensional states can also exhibit unique outstanding features. The potential of higher-dimensional quantum systems for practical applications is clearly illustrated in the demonstration of the so-called *quantum coin tossing*, where the power of higher dimensional spaces is clearly visible [15].

The amount of spatial entanglement generated depends of the SPDC geometry used (collinear vs non-collinear), the length of the nonlinear crystal (L) and the size of the pump beam (w_0). To obtain an initial estimate, let us consider a collinear SPDC geometry. Under certain approximations [16], the entropy of entanglement can be calculated analytically. Its value can be shown to depend on the ratio L/L_d , where $L_d = k_p w_0^2/2$ is the Rayleigh range of the pump beam and k_p is its longitudinal wavenumber. Therefore, large values of the pump beam waist w_0 and short crystals are ingredients for generating high entanglement [17]. However, the use of shorter crystals also reduce the total flux-rate of generated entangled photon pairs. Moreover, certain applications might benefit from the use of focused pump beams. For instance, for $L = 1$ mm, $w_0 = 200\mu\text{m}$ and $k_p = 15.7\mu\text{m}^{-1}$, one obtains $E \sim 9$ [16]. For a longer crystal of $L = 20$ mm, the amount of entanglement is severely reduced to $E \sim 5$ ebits.

We put forward here a scheme to generate massive spatial entanglement, i. e., an staggering large value of the entropy of entanglement, independently of some relevant experimental parameters such as the crystal length or the pump beam waist. This would allow to reach even

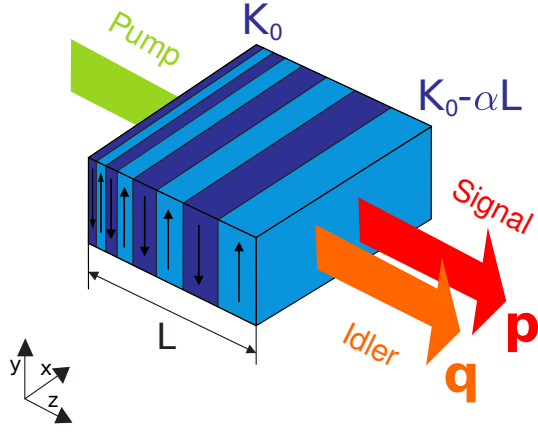


FIG. 1. Scheme of SPDC in a linearly chirped quasi-phase-matched nonlinear crystal. The pump beam is a Gaussian beam, and \mathbf{p} and \mathbf{q} designate the transverse wave numbers of the signal and idler photons, respectively. K_0 is the grating wave-vector at the input face of the nonlinear crystal, and $K_0 - \alpha L$ at its output face. The signal and idler photons can have different polarizations or frequencies. The different colors (or different direction of arrows) represent domains with different sign of the nonlinear coefficient.

larger amounts of entanglement than possible nowadays with the usual configurations used, or to attain the same amount of entanglement but with other values of the nonlinear crystal length or the pump beam waist better suited for specific experiments.

Our approach is based on a scheme originally used to increase the bandwidth of parametric down-conversion [18–20]. A schematic view of the SPDC configuration is shown in Fig.1. It makes use of chirped quasi-phase-matching (QPM) gratings with a linearly varying spatial frequency given by $K_g(z) = K_0 - \alpha(z + L/2)$, where K_0 is the grating's spatial frequency at its entrance face ($z = -L/2$), and α is a parameter that represents the degree of linear chirp. The period of the grating at distance z is $p(z) = 2\pi/K_g(z)$, so that the parameter α writes

$$\alpha = \frac{2\pi}{L} \frac{p_f - p_i}{p_f p_i} \quad (1)$$

where p_i is the period at the entrance face of the crystal, and p_f at its output face.

The key idea is that at different points along the nonlinear crystal, signal and idler photons with different frequencies and transverse wavenumbers can be generated, since the continuous change of the period of the QPM gratings allows the fulfillment of the phase-matching conditions for different frequencies and transverse wavenumbers. If appropriately designed narrow-band interference filters allow to neglect the frequency degree of freedom of the two-photon state, the linearly chirped QPM grating enhance only the number of spatial modes generated, leading to a corresponding enhancement of the amount of generated spatial entanglement.

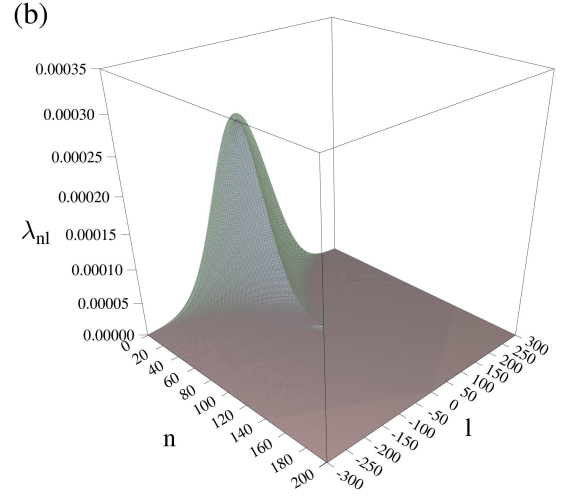
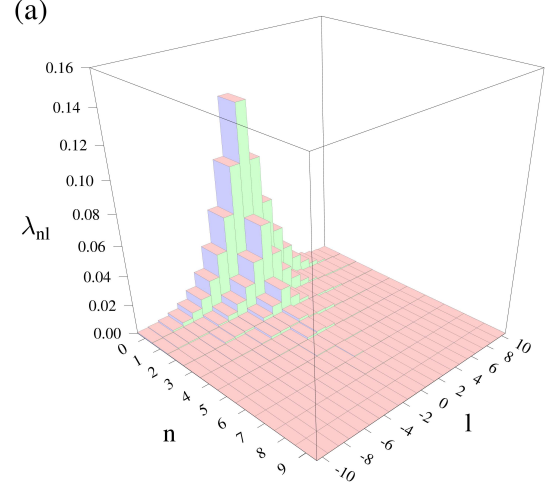


FIG. 2. Weight of the Schmidt coefficients λ_{nl} for (a) $\alpha = 0 \mu\text{m}^{-2}$ and (b) $\alpha = 10 \times 10^{-6} \mu\text{m}^{-2}$. The nonlinear crystal length is $L = 20 \text{ mm}$ and the pump beam waist is $w_0 = 200 \mu\text{m}$.

In order to determine how much spatial entanglement can be generated in SPDC with the use of chirped QPM, let us consider a nonlinear optical crystal illuminated by a quasi-monochromatic laser Gaussian pump beam of waist w_0 . Under conditions of collinear propagation of the pump, signal and idler photons with no Poynting vector walk-off, which would be the case of a noncritical type-II quasi-phase matched configuration, the amplitude of the quantum state of the generated two-photon pair generated in SPDC reads in transverse wavenumber space

$$|\Psi\rangle = \int d\mathbf{p} d\mathbf{q} \Psi(\mathbf{p}, \mathbf{q}) |\mathbf{p}\rangle_s |\mathbf{q}\rangle_i, \quad (2)$$

where \mathbf{p} (\mathbf{q}) is the transverse wavenumber of the signal (idler) photon. Ψ is the joint amplitude of the two-photon state, so that $|\Psi(\mathbf{p}, \mathbf{q})|^2$ is the probability to detect a signal photon with transverse wave-number \mathbf{p} in coincidence with an idler photons with \mathbf{q} .

The joint amplitude that describes the quantum state of the paired photons generated in a linearly chirped QPM crystal, using the paraxial approximation, is equal

$$\Psi(\mathbf{p}, \mathbf{q}) = C \sqrt{\frac{i\pi}{4\alpha}} \exp \left[-\frac{w_0^2}{4} |\mathbf{p} + \mathbf{q}|^2 - i \left(\frac{\alpha L^2}{16} + \frac{L|\mathbf{p} - \mathbf{q}|^2}{8k_p} + \frac{|\mathbf{p} - \mathbf{q}|^4}{16\alpha k_p^2} \right) \right] \times \left[\operatorname{erf} \left(\frac{3\sqrt{\alpha}L}{4\sqrt{i}} + \frac{|\mathbf{p} - \mathbf{q}|^2}{4k_p\sqrt{i\alpha}} \right) - \operatorname{erf} \left(-\frac{\sqrt{\alpha}L}{4\sqrt{i}} + \frac{|\mathbf{p} - \mathbf{q}|^2}{4k_p\sqrt{i\alpha}} \right) \right], \quad (4)$$

where erf refers to the error function. Notice that Eq. (4) is similar to the one describing the joint spectrum of photon pairs in the frequency domain, when the spatial degree of freedom is omitted [19, 20].

Since all the configuration parameters that define the down conversion process show rotational symmetry along the propagation direction z , the joint amplitude given by Eq. (4) can be written as

$$\Psi(\mathbf{p}, \mathbf{q}) = \sum_{l=-\infty}^{\infty} B_l(p, q) e^{il(\varphi_p - \varphi_q)}. \quad (5)$$

Here, we have made use of polar coordinates in the transverse wave-vector domain for the signal, $\mathbf{p} = (p \cos \varphi_p, p \sin \varphi_p)$, and idler photons $\mathbf{q} = (q \cos \varphi_q, q \sin \varphi_q)$, where $\varphi_{p,q}$ are the corresponding azimuthal angles, and p, q are the radial coordinates. The specific dependence of the Schmidt decomposition on the azimuthal variables φ_p and φ_q reflects the conservation of orbital angular momentum in this SPDC configuration [21], so that a signal photon with OAM winding number $+l$ is always accompanied by a corresponding idler photon with OAM winding number $-l$. The probability of such coincidence detection for each value of l is the spiral spectrum [22] of the two-photon state, i.e., the set of values $P_l = \int p dp q dq |B_l(p, q)|^2$. Recently, the spiral spectrum of some selected SPDC configuration have been measured [23].

The Schmidt decomposition [24, 25] of the spiral function, i.e., $B_l(p, q) = \sum_{n=0}^{\infty} \sqrt{\lambda_{nl}} f_{nl}(p) g_{nl}(q)$, is the tool to quantify the amount of entanglement present. λ_{nl} are the Schmidt coefficients (eigenvalues), and the modes f_{nl} and g_{nl} are the Schmidt modes (eigenvectors). Here we obtain the Schmidt decomposition by means of a singular-value decomposition method. Once the Schmidt coefficients are obtained, one can obtain the entropy of entangle-

to

$$\Psi(\mathbf{p}, \mathbf{q}) = C \exp \left(-\frac{w_0^2}{4} |\mathbf{p} + \mathbf{q}|^2 \right) \times \int_{-L/2}^{L/2} dz \exp \left[i \frac{|\mathbf{p} - \mathbf{q}|^2}{2k_p} z + i\alpha \left(z + \frac{L}{2} \right) z \right], \quad (3)$$

where C is a normalization constant ensuring $\int d\mathbf{q} \int d\mathbf{p} |\Psi(\mathbf{p}, \mathbf{q})|^2 = 1$. After integration along the z -axis one obtains

ment as $E = -\sum_{nl} \lambda_{nl} \log_2 \lambda_{nl}$. An estimation of the overall number of spatial modes generated is obtained via the Schmidt number $K = 1/\sum_{nl} \lambda_{nl}^2$, which can be interpreted as a measure of the effective dimensionality of the system. Finally, the spiral spectrum is obtained as $P_l = \sum_n \lambda_{nl}$.

For the sake of comparison, let us consider first the usual case of a QPM crystal with no chirp, i.e., $\alpha = 0 \mu\text{m}^{-2}$, and length $L = 20$ mm, pumped by a Gaussian beam with longitudinal wavenumber $k_p = 15.7 \mu\text{m}^{-1}$ and pump beam waist $w_0 = 200 \mu\text{m}$. In this case, the integration of Eq. (3) leads to [26]

$$\Psi(\mathbf{p}, \mathbf{q}) = C \exp \left(-\frac{w_0^2}{4} |\mathbf{p} + \mathbf{q}|^2 \right) \operatorname{sinc} \left(\frac{L|\mathbf{p} - \mathbf{q}|^2}{4k_p} \right). \quad (6)$$

The Schmidt coefficients are plotted in Fig. 2(a), and the corresponding spiral spectrum is shown in Fig. 3(a). The main contribution to the spiral spectrum comes from the spatial modes with $l = 0$. The entropy of entanglement for this case is $E = 5.1$ ebits and the Schmidt number is $K = 18.3$.

Nonzero values of the chirp parameter α lead to an increase of number of generated modes, as it can be readily seen in Fig. 2(b) for $\alpha = 10 \times 10^{-6} \mu\text{m}^{-2}$. This broadening effect is also reflected in a corresponding broadening of the spiral spectrum, as shown in Fig. 3(b). Indeed, Fig. 4(a) shows that the entropy of entanglement increases with increasingly larger values of the chirping parameter, even though for a given value of w_0 , its increase saturates for large values of α . For $w_0 = 200 \mu\text{m}$ and $\alpha = 10 \times 10^{-6} \mu\text{m}^{-2}$, we reach a value of $E = 13.47$ ebits. On the contrary, the Schmidt number K rises linearly with α , as can be observed in Fig. 4(b), for all values of w_0 . For sufficiently large values of w_0 and α , K reaches values of several thousands of spatial modes,

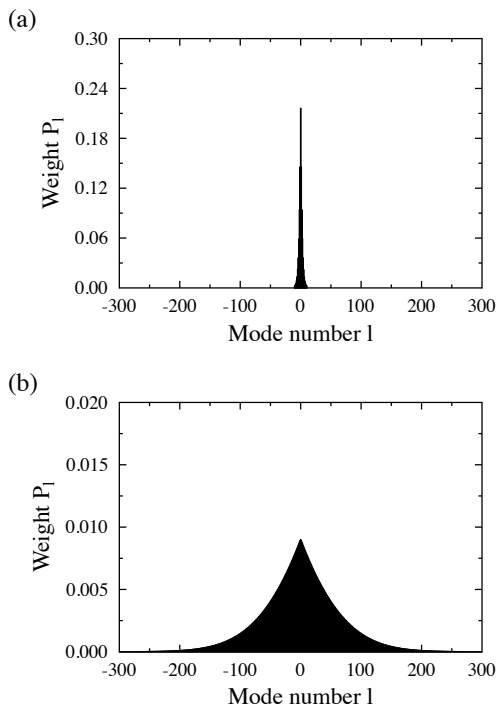


FIG. 3. The spiral spectrum P_l for (a) $\alpha = 0 \mu\text{m}^{-2}$ and (b) $\alpha = 10 \times 10^{-6} \mu\text{m}^{-2}$. The nonlinear crystal length is $L = 20$ mm and the pump beam waist is $w_0 = 200 \mu\text{m}$.

i.e. $K = 8097.76$ for the same w_0 and α . For large values of E , a further increase of E requires an even much larger increase of the number of spatial modes involved, which explain why an increase of the number of modes involves only produces a modest increase of the entropy of entanglement.

For the sake of comparison, when considering frequency entanglement, the entropy of entanglement depends on the ratio between the bandwidth of the pump beam (typically $B_p \sim 5$ MHz) and the bandwidth of the down-converted two-photon state (B_{dc}) [27]. For type II SPDC, one has typically values of $E \sim 1 - 2$ [7]. Increasing the bandwidth of the two-photon state, one can reach values of $B_{dc} > 1000$ THz, therefore allowing typical ratios greater than $B_{dc}/B_p \gg 10^8$, with $E > 25$ [28].

In conclusion, we have presented a new way to increase significantly the amount of two-photon spatial entanglement generated in SPDC by means of the use of chirped quasi-phase-matching nonlinear crystals. This opens the door to the generation of high entanglement under various experimental conditions, such as different crystal lengths and sizes of the pump beam.

QPM engineering can also be an enabling tool to generate truly massive spatial entanglement, with state of the art QPM technologies [19] potentially allowing to reach entropies of entanglement of tens of ebits. Therefore, the

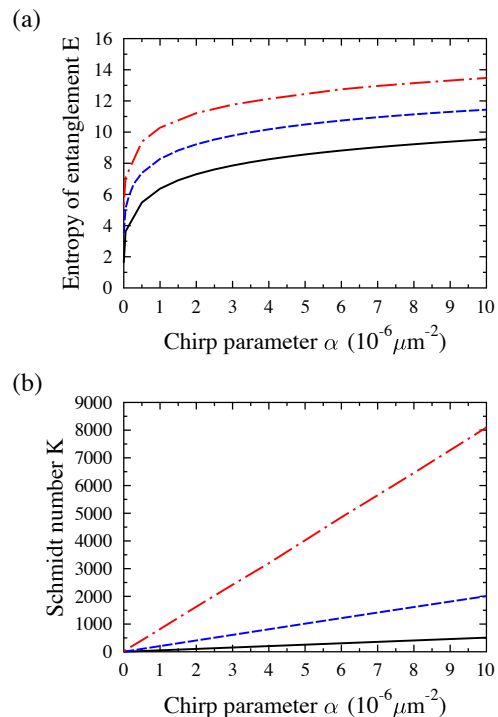


FIG. 4. (a) The entropy of entanglement E and (b) the Schmidt number K as a function of the chirp parameter α for $w_0 = 40 \mu\text{m}$ (solid black line), $w_0 = 100 \mu\text{m}$ (dashed blue line) and $w_0 = 200 \mu\text{m}$ (dotted-and-dashed red line).

promise of reaching extremely high degrees of entanglement, offered by the use of the spatial degree of freedom, can be fulfilled with the scheme put forward here. The experimental tools required are available nowadays.

The shaping of QPM gratings are commonly used in the area of non-linear optics for multiple applications such as beam and pulse shaping, harmonic generation and all-optical processing [29]. In the realm of quantum optics, its uses are not so widespread, even though QPM engineering has been considered, and experimentally demonstrated, as a tool for spatial [30, 31] and frequency [19] control of entangled photons. In view of the results obtained here concerning the enhancement of the degree of spatial entanglement, it could be possible to devise new types of gratings that turn out to be beneficial for other applications in the area of quantum optics.

This work was supported by the Government of Spain (Project FIS2010-14831) and the European union (Project PHORBITECH, FET-Open 255914). J. S. thanks the project FI-DGR 2011 of the Catalan Government. This work has also supported in part by projects COST OC 09026, CZ.1.05/2.1.00/03.0058 of the Ministry of Education, Youth and Sports of the Czech Republic and by project PrF-2012-003 of Palacký University.

-
- * jiri.svozilik@icfo.es
- [1] C. H. Bennett, G. Brassard, C. Crépeau, R. Jozsa, A. Peres, and W. K. Wootters, *Phys. Rev. Lett.* **70**, 1895 (1993).
- [2] A. K. Ekert, *Phys. Rev. Lett.* **67**, 661 (1991).
- [3] G. Ribordy, J. Brendel, J. D. Gautier, N. Gisin, and H. Zbinden, *Phys. Rev. A* **63**, 012309 (2000).
- [4] A. Serafini, S. Mancini, and S. Bose, *Phys. Rev. Lett.* **96**, 010503 (2006).
- [5] J. P. Torres, K. Banaszek and I. A. Walmsley, *Progress in Optics* **56** (chapter V), 227 (2011).
- [6] P. G. Kwiat, K. Mattle, H. Weinfurter, A. Zeilinger, A. V. Sergienko, and Y. Shih, *Phys. Rev. Lett.* **75**, 4337 (1995).
- [7] C. K. Law, I. A. Walmsley, and J. H. Eberly, *Phys. Rev. Lett.* **84**, 5304 (2000).
- [8] H. H. Arnaut and G. A. Barbosa, *Phys. Rev. Lett.* **85**, 286 (2000).
- [9] A. Mair, A. Vaziri, G. Weihs and A. Zeilinger, *Nature* **412**, 313 (2001).
- [10] J. T. Barreiro, N. K. Langford, N. A. Peters, and P. G. Kwiat, *Phys. Rev. Lett.* **95**, 260501 (2005).
- [11] E. Nagali, F. Sciarrino, F. De Martini, L. Marrucci, B. Piccirillo, E. Karimi and E. Santamato, *Phys. Rev. Lett.* **103**, 013601 (2009).
- [12] For a two-photon state with density matrix ρ_{12} , the entropy of entanglement is defined as $E = -Tr(\rho_1 \log_2 \rho_1)$, where $\rho_1 = Tr_2 \rho_{12}$ is the partial trace over the variables describing subsystem 2 of the global density matrix. The entropy of entanglement of a maximally entangled quantum state, whose two parties live in a d -dimensional system, is $\log_2 d$. Since the state of polarization of a single photon is a two-dimensional system, the maximum entropy of entanglement is 1.
- [13] D. Kaszlikowski, P. Gnacinski, M. Zukowski, W. Miklaszewski, and A. Zeilinger, *Phys. Rev. Lett.* **85**, 4418 (2000).
- [14] D. Collins, N. Gisin, N. Linden, S. Massar, and S. Popescu, *Phys. Rev. Lett.* **88**, 040404 (2002).
- [15] G. Molina-Terriza, A. Vaziri, R. Ursin and A. Zeilinger, *Phys. Rev. Lett.* **94**, 040501 (2005).
- [16] The approximation consist of substituting the sinc function appearing later on in Eq. (6) by a Gaussian function, i.e. $\text{sinc } bx^2 \approx \exp[-\gamma bx^2]$ with $\gamma = 0.499$, so that both functions coincide at the 1/2-intensity. For a detailed calculation, see K. W. Chan, J. P. Torres, and J. H. Eberly, *Phys. Rev. A* **75**, 050101(R) (2007).
- [17] S. S. R. Oemrawsingh, X. Ma, D. Voigt, A. Aiello, E. R. Eliel, G. W. 't Hooft, and J. P. Woerdman, *Phys. Rev. Lett.* **95**, 240501 (2005).
- [18] S. Carrasco, J. P. Torres, L. Torner, A. Sergienko, B. E. A. Saleh, and M. C. Teich, *Opt. Lett.* **29**, 2429 (2004).
- [19] M. B. Nasr, S. Carrasco, B. E. A. Saleh, A. V. Sergienko, M. C. Teich, J. P. Torres, L. Torner, D. S. Hum, and M. M. Fejer, *Phys. Rev. Lett.* **100**, 183601 (2008).
- [20] J. Svozilfk, and J. Peřina Jr., *Phys. Rev. A* **80**, 023819 (2009).
- [21] C. I. Osorio, G. Molina-Terriza, and J. P. Torres, *Phys. Rev. A* **77**, 015810 (2008).
- [22] J. P. Torres, A. Alexandrescu, and L. Torner, *Phys. Rev. A* **68**, 050301 (2003).
- [23] H. Di Lorenzo Pires, H. C. B. Florijn, and M. P. van Exter, *Phys. Rev. Lett.* **104**, 020505 (2010).
- [24] A. Ekert and P. L. Knight, *Am. J. Phys.* **63**, 415 (1995).
- [25] C. K. Law and J. H. Eberly, *Phys. Rev. Lett.* **92**, 127903 (2004).
- [26] S.P. Walborn, A.N. de Oliveira, S. Padua, and C.H. Monken, *Phys. Rev. Lett* **90**, 143601 (2003)
- [27] S. Parker, S. Bose, and M. B. Plenio, *Phys. Rev. A* **61**, 032305 (2000).
- [28] M. Hendrych, X. Shi, A. Valencia, and J. P. Torres, *Phys. Rev. A* **79**, 023817 (2009).
- [29] D. S. Hum and M. M. Fejer, *C. R. Physique* **8**, 180 (2007).
- [30] J. P. Torres, A. Alexandrescu, S. Carrasco, and L. Torner, *Opt. Lett.* **29**, 376 (2004).
- [31] X. Q. Yu, P. Xu, Z. D. Xie, J. F. Wang, H.Y. Leng, J. S. Zhao, S. N. Zhu, and N. B. Ming, *Phys. Rev. Lett.* **101**, 233601 (2008).